Article:

Bateman, M.D., Holmes, P.J., Carr, A.S. et al. (2 more authors) (2004) Aeolianite and barrier dune construction spanning the last two glacial-interglacial cycles from the southern Cape coast, South Africa. Quaternary Science Reviews, 23 (14-15). pp. 1681-1698. ISSN 0277-3791

https://doi.org/10.1016/j.quascirev.2004.02.001

Bateman *et al.* (2004) as published in Quaternary Science Reviews 23, 1681–1698

Aeolianite and barrier dune construction spanning the last two glacial–interglacial cycles from the southern Cape coast, South Africa

Mark D. Bateman[a],*, Peter J. Holmes[b], Andrew S. Carr[a], Benjamin P. Horton[c], Manoj K. Jaiswal[d]

[a] *Geography Department, Sheffield Centre for International Drylands Research, University of Sheffield, Winter Street, Sheffield S10 2TN, UK*
[b] *Department of Geography, University of the Free State, P.O. Box 339, Bloemfontein 9300, South Africa*
[c] *Department of Earth and Environmental Science, University of Pennsylvania, Philadelphia, PA 19104-6316, USA*
[d] *Planetary and Geosciences Division, Physical Research Laboratory, Navrangpura, Ahmedabad 380009, India*

* Corresponding author. Tel.: +44-114-222-7929; fax: +44-114-279-7912, E-mail address: m.d.bateman@sheffield.ac.uk (M.D. Bateman).

Abstract

The southern Cape region of South Africa has extensive coastal aeolianites and barrier dunes. Whilst previously reported, limited knowledge of their age has precluded an understanding of their relationship with the climatic and sea-level fluctuations that have taken place during the Late Quaternary. Sedimentological and geomorphological studies combined with an optical dating programme reveal aeolianite development and barrier dune construction spanning at least the last two glacial–interglacial cycles. Aeolianite deposition has occurred on the southern Cape coast at ca 67–80, 88–90, 104–128, 160–189 and >200 ka before the present. Using this and other published data coupled with a better understanding of Late Quaternary sea-level fluctuations and palaeocoastline configurations, it is concluded that these depositional phases appear to be controlled by interglacial and subsequent interstadial sea-level high stands. These marine transgressions and regressions allowed onshore carbonate-rich sediment movement and subsequent aeolian reworking to occur at similar points in the landscape on a number of occasions. The lack of carbonates in more recent dunes (Oxygen Isotope Stages 1/2 and 4/5) is attributed not to leaching but to changes to carbonate production in the sediment source area caused by increased terrigenous material and/or changes in the balance between the warm Agulhas and nutrient-rich Benguela ocean currents.

1. Introduction

The aeolianites found on the tectonically stable southern and eastern coasts of South Africa represent the largest Southern Hemisphere continental record of this type of deposit outside Australia (Brooke, 2001). They offer the potential to add to our knowledge of palaeoenvironments in a region particularly sensitive to past shifts in climate and ocean currents and of special interest in relation to the evolution of anatomically modern *Homo s. sapiens.* The southern Cape region of South Africa is at the current interface of the southern African winter and summer rainfall zones (WRZ and SRZ, respectively). Whilst the western winter rainfall zone, centered on Cape Town, receives its rainfall almost entirely from westerly frontal systems areas further east, including the southern Cape, experience a year-round or bimodal rainfall regime. There is recent evidence that this heterogeneity *within* the WRZ also existed during the Quaternary (e.g. Cowling et al., 1999; Meadows and Baxter, 1999; Barrable et al., 2002). The southern Cape climate and immediate sea-surface temperatures are also particularly sensitive to changes in upwelling regimes on the eastern Agulhas Bank (Cohen and Tyson, 1995). This is due to the southern Cape being at the convergence of the Benguela and Agulhas ocean currents and its location adjacent to the extensive but currently submerged Agulhas plateau. Past changes in the strength and position (which will be affected by relative sea-level change) of the Agulhas current coupled with variability in wind direction/ strength will have had a significant influence on moisture supply to coastal terrestrial environments.

The southern Cape area has a relatively rich palaeoenvironmental record from archaeological cave sites such as Die Kelders (Tankard and Schweitzer,1976; Avery et al., 1997), Boomplaas (Deacon et al., 1984), Blombos (Henshilwood et al., 2001, 2002) and Klasies River (Deacon and Deacon, 1999). These have not only provided early evidence for anatomically modern *Homo s. sapiens,* but organic remains and sediments have allowed some reconstruction of local past environments. These records contain changes in archaeological visibility, which Deacon (1995) ascribes to changing levels of aridity. The southern Cape coastline therefore is a region that not only will have been very sensitive to climatic shifts during the Pleistocene, but also in which elucidating regional palaeoenvironmental conditions during the last 200+ ka BP has important implications in terms of understanding our origins.

The southern Cape coastline has a spatially extensive and diverse range of Pleistocene aeolian deposits from which regional palaeoenvironmental conditions can be deduced. These range from extensive coastal dune fields (e.g., Alexandria coastal dune field near Port Elizabeth; Illenberger and Verhagen, 1990), barrier dunes (e.g., Wilderness cordons; Illenberger, 1996) and the aeolianites of the Waenhuiskrans Formation (Malan, 1987) to discrete aeolian units found within coastal cave stratigraphies (e.g., Blombos cave; Henshilwood et al., 2002) and pan fringing lunette dunes. However, as the review of Brooke (2001, p. 141) illustrated, the temporal control on African aeolianites is extremely poor. Whilst preliminary age estimates from the Wilderness cordons are reported in a field guide of the area (Lewis, 1999), the details of this work have to the authors knowledge never been properly published. The aims of this paper are two-fold. First, to extend the work of Illenberger (1996) and other authors on the development of the southern Cape coastal deposits with high-resolution, site-specific studies on the Wilderness seaward cordon dune and aeolianite sites from the Cape Agulhas area. This paper reports on their sedimentological properties and, through a new optically stimulated luminescence (OSL) dating programme, provides a temporal framework of their deposition. Secondly, on the basis of this record, we attempt to shed more light on the structure, development and physical properties of the dune cordons and aeolianites, and with comparison to similar records from other continents, to revisit the question of dune formation in relation to sea-level oscillations during the Upper Pleistocene.

2. Site localities

2.1. *Cordon dunes*

The section of the southern Cape coast between the towns of Wilderness and Knysna (Fig. 1c) is dominated by an impressive series of large shore-parallel fossil dune ridges or cordons reaching upto 200m above-sea-level in height (Davies, 1976, Fig. 2). Extensive accounts of the physical geography of the southern Cape and the geomorphic features of the Wilderness dune cordons have been provided by Martin (1959, 1962), Tyson (1971) and Tinley (1985). Essentially, the dunes are of parabolic form, with the trailing arms of the dune orientated parallel to the palaeowind direction, which was predominantly westerly. The Wilderness embayment, forming palaeoseacliffs, is cut into late Precambrian granites and quartzitic sediments and is possibly of Tertiary age (Potgieter, 1950; Illenberger, 1996). Within this embayment are situated older deposits, a series of lakes, and the fossil dunes which make up Illenberger's (1996) seaward, middle and landward dune cordons. A further element recognised by Illenberger (1996) is the trailing arms of a younger sequence of parabolic, ascending dunes (Tinley, 1985).

Recent large-scale sand quarrying operations at 33°59'57"S and 22°41'01"E on the N2 highway between Wilderness and Sedgefield have exposed a hitherto inaccessible sedimentary sequence in the landward flank of the seaward cordon, allowing access to the core of the dune (Figs. 1 and 2). Here, the seaward dune cordon is situated ~1.5 km inland and orientated parallel to the coastline. It reaches a height of ~100 m above-sea-level, which is ~50m less than the maximum height attained by the seaward cordon to the east of Sedgefield (Fig. 1). The seaward flank of the cordon has a mean slope angle of ~25° which is considerably less than the maximum angle of repose of vegetated sand (~34°) attained on the northern flank of the seaward cordon (Illenberger, 1996).

2.2. *Aeolianites*

Perhaps less impressive but more spatially extensive are the aeolianites found on the southern Cape coast, which include the Pleistocene aeolian-derived Waenhuiskrans Formation of the Cainozoic Bredasdorp Group (Fig. 1, Malan, 1987). These deposits have been correlated with similar deposits found in the Western and Eastern Cape coastlines; the Nahoon Formation in the Algoa Group and the Langebaan Formation in the Sandveld Group (Malan, 1990). The Waenhuiskrans Formation is a sandy, semi-consolidated, large-scale (up to 3m) trough cross-bedded aeolianite whose cross bedding shows deposition predominantly from the south-east (Malan and Viljoen, 1990). It is dominated by very coarse, well-rounded quartz grains with scattered comminuted shells and occasionally contains shows deposition predominantly from the south-east (Malan and Viljoen, 1990). It is dominated by very coarse, well-rounded quartz grains with scattered comminuted shells and occasionally contains terrestrial gastropods, as well as fragments of marine shells and foraminifera (Malan and Viljoen, 1990). The Waenhuiskrans Formation reaches thicknesses in excess of 100m in places and is extensively exposed along the coastline between Hermanus and Plettenberg Bay (Malan, 1987, 1990).

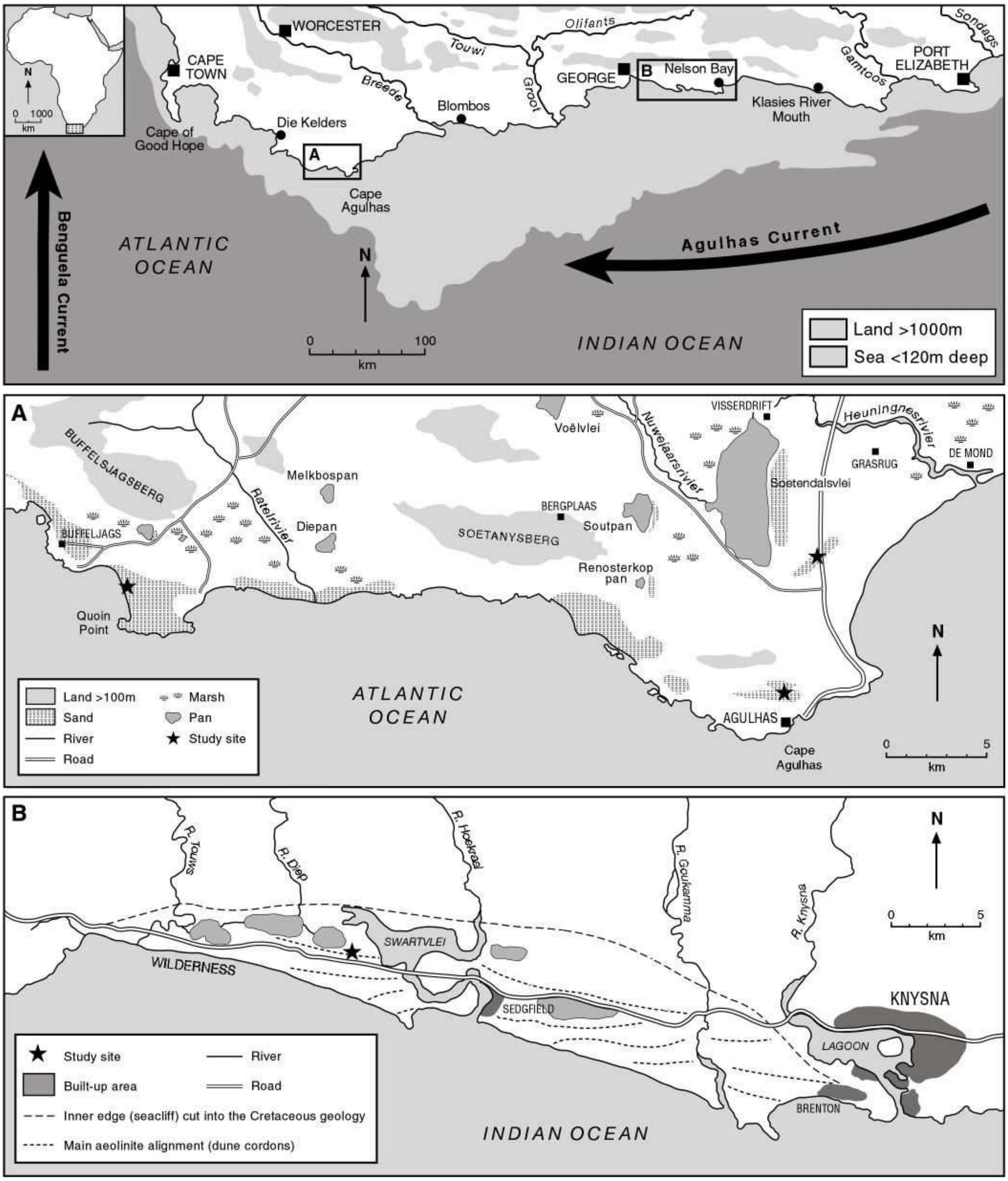

Fig. 1. Location map of the southern Cape coastline of South Africa, Wilderness Cordon dunes and sample sites.

This formation formerly extended to below-sea-level (Birch et al., 1978) and today forms eroded coastal cliffs. Unconformably overlying the Waenhuiskrans Formation are the unconsolidated wind-blown semi-stabilised dunes of the Strandveld Formation.

Three outcrops of aeolianite occurring in the Cape Agulhas area were logged and sampled. The first site is directly north of the town of Agulhas where a number of shore-parallel aeolianite ridges rise to 137masl. Large well-lithified exposures are visible at their base (15masl) whilst the crests, interdunal and shore facing areas often have upto 1m of unconsolidated sands on them. A building site near to the crest of one of the larger ridges (34°45’43”S and

Fig. 2. Wilderness seaward cordon (A) as viewed from middle cordon (B).

20 ° 00’58”E 104 m asl) *ca* 2.75km north of the present shoreline provided a 2.7m exposure. The second site is approximately 32km west of Cape Agulhas, at Hoe Walle (34°45’18”S and 19°39’01”E) where an 8m high cliff provided a complete section through the Waenhuiskrans formation (0–5.7m) and the late Middle Pleistocene Klein Brak formation (5.7– 7+m) (Malan, 1990; Malan and Viljoen, 1990). The cliff is capped by ca 30 cm of (pedogenic) calcrete and a thin veneer (1–2 m) of shifting sands. The third site (34 °44’19”S and 20 °01’39”E, 10masl) is located on the R319 Bredasdorp–Struisbaai road 10.5km north of Cape Agulhas, near Soetendals Valley (Fig. 1). Here, a 6m aeolianite exposure capped by calcrete is exposed in a road cutting. The site hosts fynbos vegetation.

3. Methods

3.1. *Field description and sampling*

At the cordon dune site two sections were cleared in the quarry. A 6.5m deep section was dug with a mechanical excavator in the upper unconsolidated sand and a second ca. 7m section was cleaned up in the more consolidated sand (Figs. 3 and 4). The aeolianite sites all used pre-existing exposures which required only hand cleaning to provide sections of 2.7m at Agulhas ridge, 4.1m at Soetendals Valley ridge and 8m at Hoe Walle. Sites were described in the field and profiles were logged and sampled using standard geomorphological and sedimentological procedures. To derive a chronology for the construction of the seaward cordon and emplacement of the Agulhas aeolianites, samples were collected for OSL dating. All OSL samples were collected in opaque PVC tubes whose ends were sealed to form a light-tight container. Sampling avoided pedogenic sediments or sediments within 30 cm of a stratigraphic boundary. The location of all samples collected is shown in Fig. 5.

Fig. 3. Exposure of lower aeolianite unit at in the Wilderness seaward cordon with (A) calcified sand with high-angle bedding, (B) iron staining of upper surface associated with inferred palaeosol.

Fig. 4. Exposure of friable unconsolidated upper sand unit with (A) silty clay lamellae at the Wilderness seaward cordon.

3.2. *Luminescence dating*

OSL samples were opened under the controlled red-light conditions of the Sheffield Centre for International Drylands Research Luminescence Laboratory and tube ends, which may have been exposed to sunlight during sampling, were discarded.

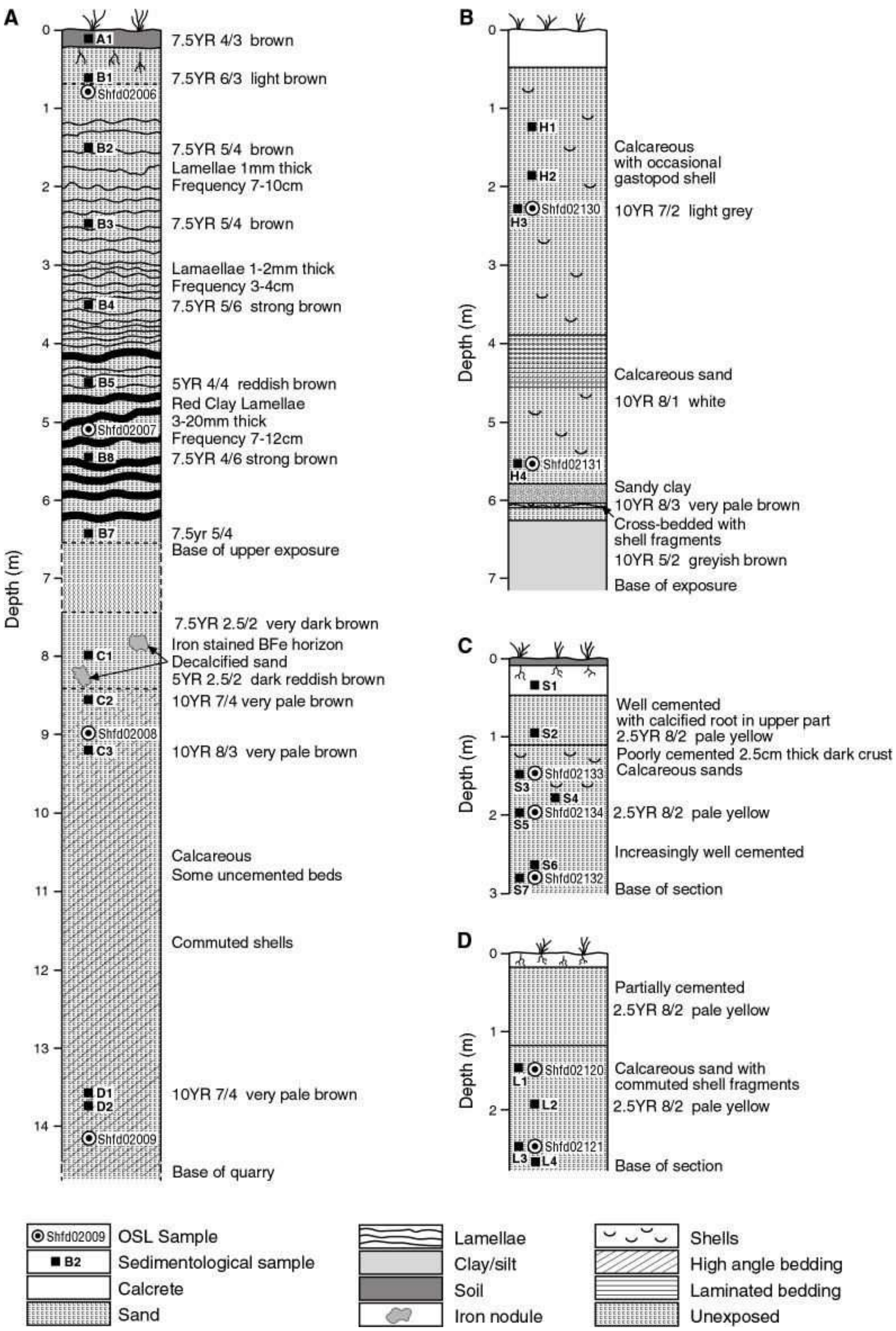

Fig. 5. Composite stratigraphy of sediments revealed through (A) Wilderness seaward cordon, (B) Hoe Walle Cliff, (C) Soetendals Valley ridge, and (D) Agulhas ridge.

The sample preparation procedure to obtain clean quartz fractions from each sample followed that of Bateman and Catt (1996). All samples were measured using an upgraded Risø TL-DA- 12 reader with optical stimulation provided by a 150W halogen lamp filtered with GG-420 and SWP interference filters and the

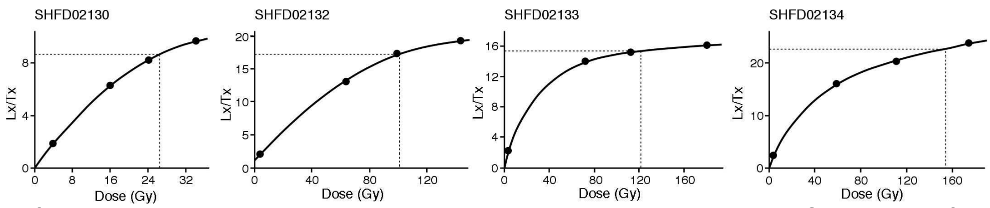

Fig. 6. Examples of equivalent dose determination based on the single aliquot regenerative dose (SAR) protocol for quartz. Note that Shfd02133 in particular is at or near saturation.

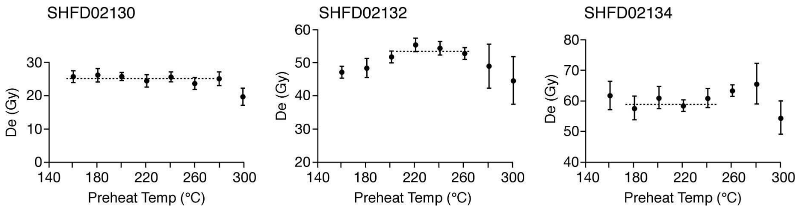

Fig. 7. Examples of preheat plateaux tests undertaken to establish most appropriate preheat temperature to use in the SAR dose protocol for southern Cape samples. Note that measurements used only a reduced point SAR protocol. Separate data, with better characterised growth curves were generated for use in age calculations.

resultant luminescence measured through a Hoya U-340 filter. The single aliquot regeneration (SAR) protocol was used to determine the palaeodose (D_e) using the OSL response to a 2.3 Gy test dose to monitor sensitivity changes (Murray and Wintle, 2000, Fig. 6). OSL measurements were made at 125°C with a stimulation time of 100 s to ensure reduction of OSL to <10% of initial OSL, thereby avoiding significant carryover on the next OSL measurement within the SAR protocol. Preheat plateaux tests (using a three regeneration point SAR protocol and a range of preheat temperatures of between 160°C and 260°C in 20°C increments) were carried out for each site to experimentally determine the most appropriate preheat to apply within the SAR protocol (Fig. 7). The preheats used varied from 180°C for sample Shfd02034, 200°C for sample Shfd02130, 220°C for samples Shfd02132 and Shfd02133, 240°C for samples Shfd02120 and Shfd02121 and 260°C for samples Shfd02006–Shfd02009. A preheat time of 10 s was used in all cases. A 160°C cutheat for the OSL response to the test dose was used for all samples. For the data used in the final age calculation, five regeneration points were measured including a replicate of the first regeneration point which was used to check the sensitivity correction procedure, through calculation of a recycling ratio, was performing adequately. This protocol worked well for all samples except sample Shfd02133 from the Soetendals Valley ridge site which appeared to be almost at saturation thus making it very difficult to construct a regenerative growth curve from which accurate interpolation between regenerative points could be made (Fig. 6). As such, the reliability of data from this sample is viewed with caution. Between 12 and 34 replicates per sample were carried out. Data from aliquots were rejected if there was a poor fit of the growth curves to the regeneration points or if recycling values fell beyond 1.0 ± 0.1. All replicate D_e data from each sample were plotted as frequency histogram, probability and radial plots and further aliquots were rejected if they appeared to deviate significantly from the normal distribution. In this way it was hoped to exclude any aliquots with a significant poorly/less-well bleached component which, if retained, would lead to an age over-estimation. Final D_e values were derived from the remaining replicate data using a weighted (by variance) mean with associated standard errors.

More detailed measurements at the single grain level were carried out on the two upper-most samples from the Wilderness cordon using the Risø TL DA-15 single grain laser luminescence reader at the Physical Research Laboratory (PRL), Ahmedabad, India. These data were used to gain an insight into the heterogeneity of the samples and to evaluate any possible incomplete bleaching problems. A focussed 532nm Nd:YVO_4 laser provided the stimulation and luminescence detection was through a U-340 filter. Approximately 2600–2700 grains were measured for each sample with a SAR protocol identical to that described above. D_e values from grains were only accepted where their recycling ratio was 1±0.15, they exhibited good growth with dose and their error on the D_e was less than 25%. Of all the grains measured, only 64 and 74 D_es for samples Shfd02006 and Shfd02007 met the above criteria. A shift in mean D_e is also noted between the single grain

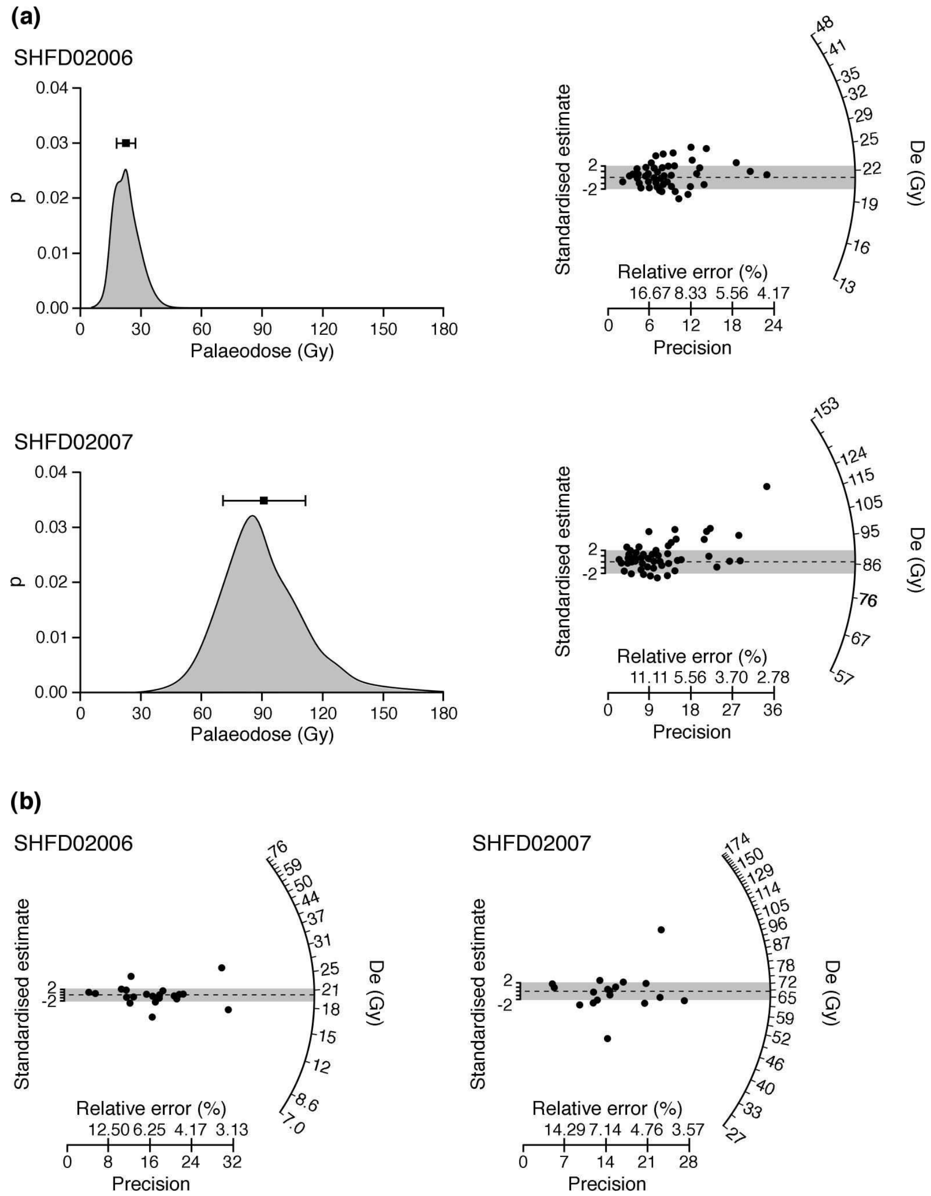

Fig. 8. OSL palaeodose data for samples Shfd02006 and Shfd02007 from Wilderness seaward cordon. (a) Single grain data plotted as probability density with the weighted mean and standard deviation above and as radial graphs, and (b) single aliquot data plotted as radial graphs.

and single aliquot data for these two samples (Fig. 8). The cause of this is not known although interlaboratory and instrument differences can be ruled out as comparisons between PRL, India and Sheffield, UK on samples produced coincident results. For the purposes of this paper, single aliquot data were used for all age calculations.

Dose rates were based on concentrations as determined by inductively coupled plasma (ICP) mass spectrometry for uranium (U) and thorium (Th) and ICP-emission spectroscopy for potassium (K) at XRAL laboratories, Canada. For the Agulhas aeolianites, the concentration values were low but still within the ICP detection limits (Th=0.01 ppm, U=0.05 ppm, K=0.01%). Dose rates for both the Hoe Walle and Soetendals Valley ridge sites were also measured using in situ gamma spectrometry. All data were converted to dose rates using the values in Aitken (1985, p. 67). Whilst the ratio of U to Th is unusual, dose rate disequilibrium problems were ruled out by comparing U and Th data for samples Shfd02132 and Shfd02133 from in situ

Table 1: Agulhas aeolianites and Wilderness cordon OSL samples: dose rate data, palaeodoses and ages.

Site	Lab Code	Depth (m)	Size Fraction (μm)	U (ppm)	Th (ppm)	K (%)	Moisture (%)	Cosmic (μGy/a)	Total Dose Rate (μGy/a)	Palaeodose (Gy)	Age (ka)
Wilderness Seaward Cordon	Shfd02006	0.80	212-250	5.0	3.7	0.2	3.7	188 ± 9	1768 ± 75	18.9 ± 0.37	**10.7 ± 0.5**
	Shfd02007	5.10	212-250	1.4	3.9	0.2	2.6	109 ± 5	901 ± 27	64 ± 1.8	**73 ± 3**
	Shfd02008	2.65	212-250	1.7	1.9	0.2	1.8	147 ± 7	868 ± 29	77.6 ± 1.6	**90 ± 4**
	Shfd02009	7.85	212-250	1.0	1.6	0.2	3.6	79 ± 4	606 ± 20	77.1 ± 2.4	**128 ± 6**
Agulhas Ridge	Shfd02120	1.5	180-212	0.4	0.4	0.1	1.1	172 ± 9	392 ± 13	62.3 ± 1.4	**159 ± 6**
	Shfd02121	2.4	150-180	0.6	0.7	0.1	3.3	153 ± 8	437 ± 13	78.3 ± 1.6	**179 ± 7**
Hoë Walle	Shfd02130	2.1	180-250	0.3 *	0.4 *	0.1 *	2.2	156 ± 8	348 ± 10	27.9± 0.4	**80± 3**
	Shfd02131	5.3	180-250	0.4 *	0.2 *	0.1*	3.5	104 ± 5	303 ± 10	26.7 ± 1.2	**88 ± 4**
Soetendals ridge	Shfd02132	2.7	150-180	1.0	0.9	0.1*	1.9	144 ± 7	551 ± 20	96.8 ± 2	**176 ± 7**
	Shfd02133	1.5	212-250	1.0	1.1	0.1*	1.3	169 ± 8	576 ± 20	119.1 ± 7	**209 ± 15****
	Shfd02134	1.9	150-180	1.0*	1.0*	0.1*	2.2	160 ± 8	565 ± 20	160 ± 3	**283 ± 11****

* = Element analysed by gamma-spectroscopy not by ICP
** = OSL data problematic therefore reliability of age questionable

gamma-spectrometry measurements, which measures daughter isotopes at bottom end of decay chains, with ICP measurements, which determines parent concentrations directly. These data gave ratios of between 0.94 and 1.05, well within the 10% measurement uncertainties used when calculating the dose rates. Values of U:Th close to unity may reflect the high marine carbonate content of the sediments. Provided that U and Th have been in these ratios since aeolianite deposition, the calculated dose rate should be valid. Palaeomoisture values were assumed to have been similar to the present day, although errors of 75% were adopted to take into account past fluctuations. The cosmic dose contribution was calculated following the algorithm set out in Prescott and Hutton (1994). The final ages, using single aliquot measurements, are presented in Table 1.

3.3. *Sedimentological properties*

Air-dried samples were routinely analysed to determine particle size, calcium carbonate content, pH and electrical conductivity. Particle size analysis for the Wilderness cordon dune samples was undertaken using a hydrometer to determine the proportions of clay and silt, and a settling column for the sand fraction. Calcium carbonate contents were determined by acid leaching using 10% hydrochloric acid (Siesser and Rogers, 1970). Particle size analysis for the aeolianite sites was carried out using a CILAS940L laser granulometer, capable of measuring sizes in the range of 0.05 μm to 2mm. Approximately 0.5–0.75 g of each sample subsample was boiled in 38% hydrogen peroxide for 20 min prior to measurement to remove extraneous organic matter. The carbonate contents of the aeolianite samples were calculated using a calcimeter, following the technique outlined by Bascomb (1974). The results of particle size analysis, pH and conductivity, and the relevant statistical parameters (Folk and Ward, 1957) are presented in Table 2a and b.

4. Description

4.1. *Morphology and sedimentology of the Wilderness seaward cordon*

The gross stratigraphy of the site comprises the fossil dune core, a weathered horizon, overlying sand and a modern soil horizon (Fig. 5 and Table 2). The core of the dune comprises a series of unweathered parallel laminated aeolianite beds with mean thicknesses upto ~60 cm, alternating with more friable strata, both of which dip at a mean angle of ~30^o on a true bearing of ~294 ^{o} (north-west) (Fig. 3). Lithologically, it comprises almost entirely medium grained very well sorted sand (Table 2) displaying little skewness. Only the upper part of the weathered horizon (sample C1) comprises more than 20% fines. Sample C3 displays a slight tail of coarser sand but this proved, on inspection, to be a function of incomplete disaggregation into primary particles, rather than an inherent grain size property. The upper stratum (~1.1m thickness) displays a weathered, decalcified zone of very pale brown (10YR 7/4) sand which is in turn capped by very dark brown (7.5YR 2.5/2), ferruginised sand. The transitions between each phase are gradual, and the original bedding structures are still visible, implying in situ post-depositional alteration. This stratum is also

Table 1. Morphometric properties of sediment samples.

Sample Details			Particle size (%)					Statistical analysis of sand fraction					Geochemistry		
Field Code	Unit Description	Depth (m)	Coarse Sand	Medium Sand	Fine Sand	Silt	Clay	Mean (Ø)	Median (Ø)	Sorting (Ø)	Skew	Kurtosis	calcium carbonate (%)	pH	Conductivity (μΣχμ^{-1})
Wilderness Seaward Cordon															
A1	Topsoil horizon	0.2	4.04	56.33	39.63	9.04	3.00	1.91	1.90	0.45	0.04	1.26	1.75	5.07	97.00
B1	Friable sand	0.6	1.98	63.15	34.87	7.76	3.00	1.88	1.86	0.39	0.10	1.18	1.13	6.62	56.80
B2	Friable sand	1.5	1.19	67.59	31.22	6.94	3.00	1.84	1.82	0.38	0.12	1.12	0.51	6.60	53.10
B3	Friable sand	2.5	1.33	62.69	35.98	3.20	2.00	1.88	1.86	0.40	0.11	1.07	0.87	6.84	49.90
B4	Friable sand	3.5	1.56	63.73	34.71	1.26	1.00	1.87	1.85	0.39	0.08	1.07	0	6.31	49.50
B5	Friable sand	4.5	2.34	73.29	24.37	1.74	0.00	1.76	1.74	0.38	0.09	1.10	0.23	6.56	50.80
B6	Friable sand	5.5	1.51	55.34	43.15	5.66	2.00	1.96	1.94	0.40	0.11	1.19	0.88	7.05	52.20
B7	Friable sand	6.5	1.00	61.39	37.61	6.74	4.00	1.90	1.88	0.38	0.10	1.10	0.63	7.13	78.30
B8	Lamellae*		1.38	65.69	32.93	6.78	8.00	1.86	1.85	0.36	0.09	1.11	0.52	7.36	75.70
C1	Weathered aeolianite	8.1	1.00	52.58	46.42	4.30	16.00	1.98	1.97	0.30	0.05	1.06	1.62	7.80	110.70
C2	Weathered aeolianite	8.6	1.11	58.88	40.01	2.16	0.00	1.92	1.92	0.35	0.01	1.07	23.81	8.95	67.80
C3	Aeolianite	9.3	6.87	63.47	29.66	2.96	0.00	1.78	1.80	0.46	-0.12	1.27	22.74	9.28	149.40
D1	Aeolianite	13.7	1.40	53.54	45.06	0.00	0.00	1.96	1.96	0.34	-0.04	1.07	22.98	9.51	69.60
D2	Friable sand lens	13.8	3.85	71.81	24.34	2.44	0.00	1.96	1.96	0.34	-0.04	1.07	23.54	9.54	80.40
Soetendal Ridge															
S1	Indurated calcrete	30	17.1	21.2	42.6	16.6	2.5	1.89	2.1	0.88	-0.24	1.06			
S2	Aeolianite	90	19.2	23.6	44.7	11.2	1.4	1.84	2.06	0.91	-0.18	0.85			
S3	Aeolianite	1.5	17.0	23.3	50.2	8.0	1.5	1.94	2.17	0.87	-0.28	1.26			
S4	Aeolianite	1.8													
S5	Aeolianite	1.9	18.7	9.9	60.9	9.2	1.3	2.07	2.40	0.95	-0.36	1.09			
S6	Aeolianite	2.5													
S7	Aeolianite	2.7	19.6	21.0	46.1	11.5	1.8	1.91	2.13	0.93	0.24	0.82			
Agulhas Ridge															
L1	Aeolianite	1.5	16.4	27.5	46.2	8.7	1.2	1.72	1.87	0.77	-0.18	0.95			
L2	Aeolianite	1.9	17.3	29.4	45.6	6.8	0.9	1.71	1.84	0.78	-0.16	0.87			
L3	Aeolianite	2.4	15.8	15.9	56.8	10.1	1.7	1.94	2.18	0.91	-0.29	0.96			
L4	Aeolianite	2.5	16.5	8.6	59.3	13.5	2.1	2.05	2.37	0.96	-0.35	0.90			
Hoë Walle															
H1	Aeolianite	1.3	19.2	22.7	34.4	19.3	4.4	1.66	1.79	0.84	-0.14	0.72			
H2	Aeolianite	1.8	21.3	31.9	29.5	14.4	3.0	1.67	1.81	0.78	-0.19	0.74			
H3	Aeolianite	2.1													
H4	Aeolianite	5.3	19.4	33.1	40	6.8	0.8	1.65	1.78	0.70	-0.16	0.80			

* sampled from individual lamellae, then aggregated and analysed as a whole

characterised by numerous solution pipes, with depths of up to ~30 cm which have subsequently been infilled by sand or soil. Mineralogically, the aeolianite comprises ~75% silica and ~25% calcium carbonate. However, in the decalcified uppermost 60 cm of the deposit, the calcium carbonate component falls to ~2% (Table 2). With the exception of the decalcified sample C1, which is slightly alkaline (pH 7.8), the aeolianite samples are strongly alkaline, with pH ranging from 8.95 up to 9.54. Conductivity values are low, implying a dearth of ionisable salts. The true vertical extent of the deposit is not known as the floor of the quarry does not coincide with the underlying bedrock.

Unconformably overlying the aeolianite of the dune core is a massive, apparently uniform sequence of cohesive, well-sorted, slightly positively skewed, medium-grained but friable sand (Fig. 4, Table 2). This sequence is not continuous across the whole cordon dune, but appears to have accumulated on the seaward margins of the aeolianite. Mineralogically, the sand comprises almost entirely silica and the conductivity values are generally low. There is no stratigraphic evidence of individual beds or transitions between strata. However, with the exception of the uppermost ~1m of the exposure, there are numerous strong brown (7.5YR 4/6) wavy silt/clay-rich lamellae (lamellae contain ~15% fines compared to 10% fines in the uppermost zone of friable sand). These lamellae are particularly prominent, with thicknesses of up to 1 cm in the basal 2m of this phase. Although not visually apparent in the field, the particle size data indicates differences between the top 4 m (samples B2–B5) and lower 3m of sand (samples B6–B7). Samples below 4.5 m, which carefully excluded lamellae, comprise more fine sand (average of 40% compared with 32%) and enhanced amounts of fines (average of 9% compared to 5%). Whilst the uppermost strata are slightly acidic and the basal strata are slightly alkaline, implying a degree of leaching not inconsistent with their position within the profile, both calcium carbonate and pH values increase between samples B5 and B6. Reddening associated with mobilisation of iron oxide was also noted for the sand around 4–5 m. Based on this evidence, it is suggested that the upper friable sand may represent two discrete aeolian sand units.

The friable sand phase is capped by a veneer of brown (7.5YR 4/3), sandy and structureless topsoil. The transition between the soil and the underlying sand is gradual, implying in situ development of the soil. Where the friable sand phase is absent, the topsoil directly overlies the weathered, decalcified aeolianite. The soil contains ~12% fines, and the sand is classified as medium-grained and well sorted (Table 2). It is significantly more acidic, with a pH value of 5.07, being not inconsistent with the podzolic A horizons of the region. Conductivity is low. Mineralogically it comprises less than 2% calcium carbonate (Table 2). It contains very few rootlets and little organic debris.

4.2. Morphology and sedimentology of the Agulhas aeolianites

The stratigraphy revealed in the 2.70m exposure on Agulhas ridge comprises two principle units (Fig. 5d). The upper 1.2–1.4m comprises of variably cemented, carbonate-rich sands of which the upper 20 cm are particularly indurated, forming a pedogenic calcrete cap. This upper unit is strongly karstic in appearance, with soil filled solutional hollows commonly reaching a depth of 0.5 m. Below this the sand is generally less well cemented. The lower unit comprises uniform, unconsolidated, highly calcareous (65–78%) medium sands. The sediments from this lower unit generally contain 45–60% fine sand, are moderately sorted and negatively skewed. Samples L3 and L4 are much finer, with means of 1.9 and 2.05Ø, respectively, compared to means of L1 and L2 of 1.72 and 1.71 Ø. L3 and L4 are also less well sorted and more negatively skewed. These differences are interpreted as indicating the existence of two subunits; a calcareous sand with comminuted shell fragments and a calcareous sand. The particle size distributions are not characteristic of typical aeolian sediments and there is a lack of bedding structure. However, the morphology of the Agulhas ridge as one of many shore-parallel ridges, its position relatively close to the present-day coast and presence of shell fragments in its sediments is consistent with it being interpreted as a fossil cordon dune.

At the Soetendals Valley ridge site, the upper 0.5m consists of a well-indurated pedogenic calcrete, beneath which there is a 0.5–1.0m thick unit of sands with occasional calcified root casts and animal burrows (Fig. 5c). The lower 2–3m comprises calcareous medium sands cemented to varying degrees which displays no clear bedding structures but does contain shell-rich lenses in the upper part. The carbonate content of the ridge is typically 50–65% with no discernible trends with depth. This is lower than the other two sites in the Agulhas area, but still significantly higher than the aeolianite units in the Wilderness cordon. The presence of shell and shell fragment rich lenses suggests that there is possibly considerable variation in carbonate content throughout the dune. The sediments are generally dominated by fine sand (42–50%), with minor components of medium/coarse sand (17–22%) and silt (8–17%), are moderately sorted and negatively skewed. The upper three (S1–S3) and lowest two samples (S6, S7) cannot be differentiated on the basis of the particle size data but S4 and S5 show a significant change of the medium/fine sand faction towards being much finer and are more positively skewed. Such results are suggestive that the lower unit as shown in Fig. 5 should be subdivided into three; a poorly cemented calcareous sand with shells, a poorly cemented calcareous sand and a well-cemented calcareous sand. The gross morphology the feature which was sampled is that of a linear ridge ca 1 km long, 300m wide, and upto 10m high. The ridge is orientated northeast–southwest, parallel to the present-day shoreline at Struisbaai located 4.75km to the west. As such, it is interpreted as a fossil coastal cordon dune.

The four-fold stratigraphy of the cliff section at Hoe Walle is illustrated in Fig. 5b. The upper 0.3–0.5m comprises a well-indurated calcrete pedogenic caprock with abundant solutional hollows. The sediments down to a depth of 3.8m are structureless, uniform white/buff (10YR7/2) in colour, and comprised of highly calcareous (71–80%) medium sands with occasional (often intact) gastropod shells. Sediments from this unit are dominated by moderately sorted sand with less than 23% silt or clay. The unit below is much more compacted, with laminar bedding 3–5 cm thick in the upper 0.3–0.4m. This unit is composed of white (10YR8/1) calcareous medium sands with occasional gastropod shells and recemented calcretic debris (up to 40 cm a-axis). This is the most calcareous unit of all the sampled sites (81% carbonate). Sample H4 from this unit contains much less fine material (8% compared to the 17–23% of samples from the overlying unit) and is dominated more by fine sand (40% compared to 29–34% of the overlying samples). It is also slightly better sorted (0.70). Below this unit are the silty clays of the Klein Brak Formation. The lack of morphological expression of the aeolianites exposed around Hoe Walle and the lack of structure for much of the aeolianite, with only occasional laminated bedding is interpreted as indicating aeolianite formation as part of a low-angle sheet rather than within dunes.

5. Chronology

5.1. Chronostratigraphy of the Wilderness seaward cordon

Ages of 128±6 ka (Shfd02009) and 90±4ka (Shfd02008) from the aeolianite indicate formation of the main seaward dune ridge occurred during the Upper Pleistocene within Oxygen Isotope Stages (OIS) 5e–5b. Illenberger's (1996) assertion that the seaward cordon of Eemian age is therefore correct. An age of 73±3ka (Shfd02007), correlating with the transition from OIS 4 to 5, was obtained within the unconsolidated sand unit directly above the weathered horizon. This weathered horizon represents a distinct depositional hiatus which occurred sometime within ca 90–73 ka BP (OIS 5a). Subsequent sedimentation recommenced under somewhat different environmental conditions. An age of 10.7±0.5 ka (Shfd02006) from the uppermost unconsolidated sand unit implies sand accumulation occurred around the start of the Holocene. It is not possible to interpret whether aeolianite deposition/formation within the ca 35+ ka identified from the lower OSL ages (Shfd02009 and Shfd02008) was episodic or continual. No evidence of incipient palaeosols or weathering horizons were found on bedding boundaries. Nevertheless, given the high preservation potential of sand, the magnitude of the cordon dunes, and the rapidity with which dune building occurs, it seems less likely that B5m depth of sand represents 35 ka of sand accumulation. The single grain data for sample Shfd02007 (Fig. 8a) show a tail of high palaeodoses similar to those obtained from the underlying basal aeolianite perhaps indicating that some sediment from the lower unit was locally recycled, without full bleaching, during the deposition of the lower friable sand unit. This would support the hypothesis of episodic deposition of the lower aeolianite unit. The individual beds within the aeolianite, both cemented and uncemented, could be interpreted as the product of episodic deposition followed by deflation, erosion and reworking of sand. Local recycling and mobilisation of sediment at the beginning of a period suitable for aeolian activity would remove any evidence of leaching or palaeosols that had developed during a quiescent period (Kocurek, 1998). Preservation of aeolian sediment is more likely at the end of an aeolian phase when less sediment mobilisation/reworking occurs due to, e.g., rising groundwater, sea levels or conditions favourable to cementation (Kocurek, 1998). A similar argument was put forward by Thomas et al. (2000) to explain the lack of sedimentary evidence for episodic deposition of Kalahari dunes. Whilst, measurements of OSL at the single aliquot level of Shfd02007 will have undoubtedly incorporated these less-well-bleached grains as illustrated by the single grain data, the selection criteria adopted (see luminescence section) will have mitigated some of these effects with the remainder contributing to the uncertainties associated with the data for this sample.

Both single grain and single aliquot OSL palaeodose data for the upper unconsolidated sand (Shfd02006, Fig. 8) show a good normal distribution indicative of well sunlight bleached sand grains prior to deposition, which have had no post-depositional disturbance. These data also support the differentiation of the upper friable sand into two units, with no overlap in the palaeodose values measured for the two samples. The development of lamellae post-dates the deposition of both sand subunits and must be of Holocene age.

5.2. *Chronostratigraphy off the Agulhas aeolianites*

At Agulhas Ridge the OSL ages are 159±6ka (Shfd02120) and 17977 ka (Shfd02121). The former falls within OIS 6d/e whilst the latter coincides with the transition from OIS 7 to OIS 6. As the base of the unit was not exposed, dune initiation could have begun earlier. The switch from a calcareous sand subunit to a calcareous sand with comminuted shell fragments subunit does occur over a significant time period and may reflect changes in environmental conditions and or sediment source. No ages are available for the overlying unit at this site.

The OSL ages derived for Soetendals Valley Ridge are 209±15, 283±11 and 176±7 ka (Shfd02133, Shfd02134, Shfd020132). These ages clearly do not coincide with the stratigraphy with an age reversal at depth. Some difficulty was experienced in measuring the OSL from the upper sample (Shfd02133) as it was at or near saturation (Fig. 6). No such explanation can be offered for Shfd02134 which showed good reproducible OSL growth curve characteristics and the distribution of D_e values appeared normal (Fig. 6). Given the questionable reliability of these two ages and to err on the side of caution, only the OSL age from Shfd02132, which has a good OSL growth curve and was highly reproducible, has been adopted for the purposes of subsequent discussion. Based on this age the Soetendals Valley ridge was accreting at least around OIS 7/6, which is coincident with the ages derived from the Agulhas ridge aeolianites.

At Hoe Walle the lower aeolianite unit dates to 88±4 (Shfd02131). This correlates with OIS 5b and possibly indicates that the underlying estuarine clays (which are associated with the Klein Brak Formation (Malan and Viljoen, 1990)), relate to the high sea levels and therefore high water tables associated with OIS 5e. An OSL data of 80±3 ka (Shfd02130) was obtained from midway up the uppermost aeolianite unit at this site which correlates with the transition from OIS 5a to 5b. The difference in age between the two OSL ages conforms to the site stratigraphy and clearly indicates at least two depositional phases at this locality.

5.3. *Correlation with regional aeolian activity*

The new OSL chronology for the Wilderness seaward cordon and Agulhas aeolianites shows that there has been some synchronicity along the coastline with the Wilderness cordon dunes being constructed at a similar time to the aeolianites found at Hoe Walle. Illenberger (1996) assigned part of the middle cordon dune at Wilderness to OIS 7 which would tie in with the cordon dune construction found at Agulhas and Soetendals Valley. Based on the new OSL data, all the aeolianites are older than 70 ka and can be clustered into four phases ca 73–80, 88–90, 128, 160–180 ka before the present (Fig. 9). Some supporting evidence for such a division can be found in the published literature. Recent work from the Western Cape aeolianites shows that these started to form prior to 118718, around 103–107 ka and by 7579ka (Roberts and Berger, 1997), while Shaw et al. (2001) assigned a luminescence age of 185722 ka to the aeolianites at Cape Point. Further east, a uranium series age of 182718 ka was obtained from an aeolianite core of a coastal dune at Isipingo, south of Durban (Ramsay and Cooper, 2002). Samples collected from a calcarenite at Nahoon Point near East London and from an unspecified location in a ‘‘near coastal dune in the Wilderness area’’ (Vogel et al., 1999, p. 730) luminescence dated to 75.479.4 and 67.378.9 ka, respectively (Vogel et al., 1999). In a conference abstract, Illenberger et al. (1997) presented preliminary feldspar luminescence ages (no errors given) from the Wilderness cordons (115, 200 ka) and from dunes at Cape Recife (184 ka) and Algoa Bay (154 ka) of which at least three fall within the proposed clusters of aeolianite deposition. At Blombos cave (Fig. 1) Aeolian strata separating the Middle and Late Stone Age strata OSL dated to 6975ka (Henshilwood et al., 2002). Comparison with the global aeolianite record also shows island aeolianite deposition on Bermuda and Bahamas occurred at OIS 5a, 5e, 7 and beyond, whilst widespread continental aeolianite deposition likewise occurred in southern and Western Australia during OIS 5c, 5e, 7 and beyond (Brooke, 2001). Corroborative regional evidence for Holocene aeolian activity as found at the Wilderness seaward cordon can be found from the extensively dated Alexandria coastal dunefield near Port Elizabeth (Illenberger and Verhagen, 1990), from dunes at Langebaan of the Western Cape (Roberts and Berger, 1997) and from vegetated dunes on the Agulhas Plain (Carr pers.com.). Fig. 9 shows that by combining previously published ages with the new OSL chronology from the southern Cape at least five phases of aeolianite deposition extending back to the penultimate interglacial can be identified. These phases occur at ca 67–80, 88–90, 104–128, 160–189 and >200 ka.

6. Sediment provenance

Both the Agulhas aeolianites and the aeolianite found in the core of the seaward cordon at Wilderness are carbonate rich (50–80% and 20–25%, respectively). The dispersion of this carbonate throughout the sediments rather than at discrete horizons or as nodules makes a pedogenic origin for these carbonates unlikely. All three Agulhas aeolianite sites exhibited shell fragments within the aeolianites and

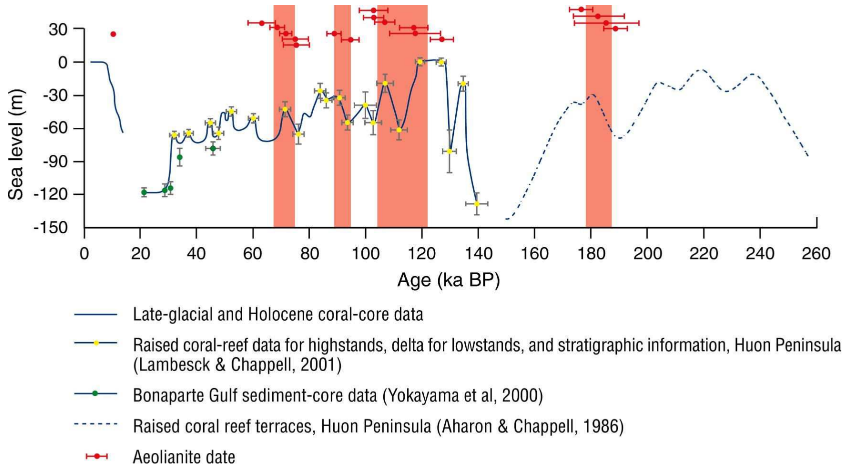

Fig. 9. Ages from aeolian sediments on the southern Cape, South Africa compared to the relative sea-level curve for the penultimate and last glacial cycle for the Huon Peninsula supplemented with observations from Bonaparte Gulf, Australia. Error bars define the upper and lower limits (modified from Lambeck et al., 2002). Aeolianite age data are from Wilderness seaward cordon (this paper, Vogel et al., 1999), Cape Agulhas aeolianites (this paper), Blombos Cave (Henshilwood et al., 2002), Western Cape aeolianites (Roberts and Berger, 1997; Shaw et al., 2001) and Eastern Cape aeolianite (Vogel et al., 1999; Ramsay and Cooper, 2002). Shading relates to mean71 standard deviation of clusters of ages.

shells and comminuted shell fragments appear relatively common within the aeolianites reported from elsewhere (e.g., Malan, 1989). The occurrence of foraminifera tests and other marine shells (Siesser, 1970) all point to a marine source for the aeolianites. Detailed studies of the offshore sedimentary record show that sediment on the Agulhas bank has an average of ca 30% intergranular carbonate and 60% carbonate grains including fossils (Siesser, 1970). Thus a marine provenance for the sediments seems likely.

Unlike the aeolianite dune core, there is no evidence of cementation of the upper sand unit on the Wilderness cordon dune. Elsewhere along the southern Cape coast many of the dune systems which form part of the Strandveld Formation are also carbonate poor. This absence of calcium carbonate either reflects a change in sediment provenance or post-depositional leaching. Leaching is discounted as the upper sediment at the Wilderness seaward cordon does not show even residual evidence of calcification and lamellae there indicate a subtle concentration of fines within the sediment, rather than wholesale leaching. The absence of calcium carbonate (Table 2) may imply a change in sediment provenance or changes in offshore carbonate production. Illenberger (1988) noted the significance of the Sundays estuary as a source of sediment for the Algoa dunefield. A number of rivers debouch from the southern slopes of the Outeniqua range dissecting the Wilderness dune cordons and they could have acted in a similar fashion. However, in some places parabolic forms climbing up the seaward side of the seaward cordon indicate sediment supply for the most recent dunes from the seaward side rather than directly from rivers. Increased fluvial discharge of terrigenous classic sediment would have reduced the off-shore production of Heterozoan carbonate. However, currently the southern Cape coast is classified as sediment-starved, with only 17.9% of sediment supplied to the continental shelve coming via rivers (Dingle et al., 1987). Additional changes to carbonate production could have been caused by changes in the relative strength and position of the confluence of the Benguela (cold) and Agulhas (warm) ocean currents which supply nutrients and high carbonate-producing biota, respectively. A second possibility is that the carbonate poor, friable sediments are formed from sediment formerly exposed and pedogenically leached on the coastal plain during a hypothermal sea-level low stand.

7. Does dune formation occur during glacials or interglacials?

The characteristics of the sand and of the morphology at all the sites are consistent with Aeolian emplacement either as dunes or as sand sheets, with the sediment being derived from the coastal plain. However, the exact association between barrier dune and coastal aeolianite formation on the one hand, and sea-level and coastline fluctuations on the other is still subject of debate (e.g., Brooke, 2001). In some areas, e.g., the Coorong coastal plain of south Australia, detailed chronostratigraphic work has shown that deposition of large coastal dunes/aeolianites occurred during interglacial and interstadial sea-level highstands. However elsewhere, including within Australia, aeolianites have been reported as being of glacial age (e.g., Zhou et al., 1994; Frechen et al., 2001). In Brooke's (2001) database of global aeolianite deposits, all the entries from South Africa lacked good temporal control. The OSL framework outlined above helps to address this problem, also noted by Ramsay and Cooper (2002, p. 84), and allows some insight into the relationship of the South African coastal aeolianites and palaeoenvironmental changes.

Tankard and Schweitzer (1974), Dingle and Rogers (1972a) and Tinley (1985) proposed a scenario for the southern and south western Cape where, during periods of marine regression, the Agulhas Bank, which here forms the continental shelf, was exposed and amenable to aeolian deflation, thus ensuring a supply of windblown sand. By way of contrast, Barwis and Tankard (1983) argued that vegetation would have rapidly invaded the exposed shelf, thus reducing the effectiveness of wind transportation. Illenberger (1996) concurred, suggesting that the Wilderness dune cordons formed during sea-level highstands associated with interglacials, and that sea levels were close to present levels. However, a point that has previously been largely overlooked is that the formation of aeolianite is a two phase process. Firstly, conditions must favour largescale entrainment and deposition of calcareous sand. Secondly, subaerial conditions favourable to cementation of the sand must prevail. Another problem which requires explanation is that the highstand of the present interglacial has not seen aeolianite deposition, rather the building of unconsolidated sand dunes, e.g., the Strandveld Formation. This Holocene dune accretion appears to be occurring simultaneously with erosion of aeolianite in the Wilderness area, as well as along the southern Cape coast towards De Hoop, Hoe Walle, around Cape Point (Shaw et al., 2001) and at Langebaan on the Cape west coast (Roberts and Berger, 1997).

Critical to understanding this is the timing and extent of sea-level changes over the last 250 ka, how these changes affected the southern Cape coastline and the distance of the aeolianites/cordon dunes from sediment sources. At a global scale, major sea-level cycles have occurred at intervals of ca 100 ka over the past ca 800 ka with a maximum amplitude of 120–140 m. Superimposed on these cycles are lesser cycles of a few tens of thousand years and shorter (Lambeck et al., 2002). Direct, accurate and high-resolution records of past sea levels exist for only the last glacial, although evidence points to a sea-level highstand during the interglacial timed at 200 ka (e.g., Chappell and Polach, 1991; Pirazolli et al., 1991; Chappell et al., 1996; Bard et al., 2002). Ramsay and Cooper (2002) described the Late Quaternary sea-level changes for a 180km stretch of coastline in eastern South Africa. Although not without problems, e.g., use of wood fragments as index rather than limiting points and combination of uncalibrated radiocarbon chronologies with those of uranium series, evidence from South Africa broadly corresponds to the records from the Caribbean (Ramsay, 1995; Illenberger, 1996; Ramsay and Cooper, 2002).

To elucidate further the relationship between dunes and sea levels, the chronometric framework established above and previously published coastal aeolian dates from the region (Roberts and Berger, 1997; Vogel et al., 1999; Shaw et al., 2001; Henshilwood et al., 2002; Ramsay and Cooper, 2002) were overlain on the relative sea-level curve for the Huon Peninsula over the penultimate and last glacial cycle (Aharon and Chappell, 1986; Lambeck and Chappell, 2001). This was supplemented with observations from Bonaparte Gulf, Australia (Yokoyama et al., 2000) (Fig. 9). The sea-level highstand which occurs around 200 ka and thought to be -3m compared to today (Ramsay and Cooper, 2002), broadly coincides with the aeolianite phase of >200 ka. Aeolianite deposition between 160 and 188 ka occurs within the transition from substage OIS 6f to the interstadial highstand of substage OIS 6e. The aeolianite deposition between 104–128 and 88–90 ka coincide with OIS 5d and the latter phase of OIS-5b, respectively. Indeed, the aeolianite phase 104–128 ka encompasses the end of the last interglacial (substage OIS 5e), when sea levels were a few metres higher than modern levels at ca 130 ka BP (Illenberger, 1996). It thus forms a possible analogue for the termination of the Holocene. During the stadials OIS 5b and OIS 5d, sea levels were as much as 40–60m below present levels (Lambeck and Chappell, 2001) although evidence presented by Ramsay and Cooper (2002) suggests sea levels during OIS 5b–5c may have been around +4m above present levels. The last phase of aeolianite deposition (68–80 ka) occurs at the OIS 5/4 boundary. OIS 4 corresponds to the period leading into the maximum glaciation and represents a time of stadials, of increasing intensity, punctuated by brief interstadials. OIS 3 is characterized by rapid fluctuations in climate and ice-volume and five highstands have been identified, centered on 32, 36, 44, 49– 52 and 60 ka ago with sea levels between -70 and -40m (Lambeck and Chappell, 2001). OIS 2 includes the LGM followed by a period of rapid ice decay when approximately 50 million km^3 of ice melted from the land-based ice sheets, raising global sea level in regions distant from the major glaciation centres, such as South Africa, by about 110–130m (Dingle and Rogers, 1972b; Illenberger, 1996; Barrable et al., 2002; Ramsay and Cooper, 2002). The past 12,000 years define OIS-1 or the Holocene, when ice volumes and climate were largely similar to those of today (Lambeck et al. 2002).

Although hampered by the level of precision associated with the chronology, two observations can be made of the apparent relationship of aeolianite deposition to sea level. Firstly, it is clear that a significant amount of aeolian deposition occurred after the high sea stand associated with the Eemian. Secondly, dunes and aeolian sediments appear to have been deposited when sea levels were rapidly changing. Such observations are in concordance with Roberts and Berger (1997) who argued, logically, that sea levels must have been falling in order to preserve the human footprints found within the Langebaan aeolianite of the Cape west coast. That aeolian sedimentation occurred during periods postdating interglacials also explains why many of the aeolianites and cordon dunes found on the present-day coastline are being eroded, as sea levels would have been marginally lower than the present-day whilst they were being deposited. Fairbridge (1995; cited in Brooke, 2001) proposed a similar model for Western Australian aeolianite formation, linking their deposition to abrupt sea level drops and an arid climate with strong onshore winds.

The great thickness of the southern Cape aeolianites may in part be attributed to them containing older deposits as yet undated. It may also be explained by examination of the effects of sea-level fluctuations on the southern Cape coastline. Barrable et al. (2002), using present-day topography and bathymetry, showed that at the last glacial maximum (LGM) lower sea levels would have exposed the Agulhas Bank, placing the coastline approximately 80km further south than the present-day Cape Agulhas. As soon as sea levels rose above -75 m, the exposed coastal shelf was reduced in width by at least two-thirds (Van Andel, 1989). Sea levels in the period 70–95 ka were nowhere near as low as at the LGM and included within this period are a number of interstadials in which sea level rose to be relatively close to that of the present day. This would have been particularly the case east of the Agulhas plateau where the coastal platform initially shelves more quickly (Dingle and Rogers, 1972a). The effect of such rises means that the sea would have returned to within a few kilometres of the present-day coastline on a number of occasions (Van Andel, 1989) allowing sediment accretion to repeatedly occur at these same localities. Thus Illenberger's observation that sand deposition rarely occurs more than 3 km inland may still be satisfied even if deposition is occurring in post-interstadial high-stand periods. This would account for the subunits of different ages found within aeolianites, e.g., at Hoe Walle, and the building up of the geomorphologically impressive Wilderness cordon dunes. It also fits well with the archaeological record from Blombos which shows human occupation in the Middle Stone at 77±6ka, aeolian deposition at 69±5 ka and then resumption of human occupation associated with the Late Stone Age (Henshilwood et al., 2002). Further evidence for cordon dune construction only near the littoral zone comes from the reporting of a complex of submarine barrier like dune ridges found off the southern Cape coast. These occur between -130 and -112m coincident with where sea levels would have been for a considerable period of time during the LGM low-stand (Van Andel, 1989). Other submarine dune complexes have been reported off the Wilderness area coastline at -40 and -50m (Birch et al., 1978), which again could relate to dune construction associated with other interstadial sea-level high stands within OIS 3 in which sea levels transgressed but not sufficiently high enough for aeolian sediments to be recorded at the present-day coastline.

8. Synopsis and conclusions

The OSL dating combined with previously published data has established for the first time a regional chronology for the coastal aeolianites of the southern Cape, which spans two glacial–interglacial cycles and redresses the lack of chronological control for the African aeolianite as reviewed by Brooke (2001). The majority of the sedimentary record examined probably relates not to deposition during interglacial highstands but to post-interglacial periods (interstadials) when sea levels were fluctuating and climatic conditions were cooler and wetter, and therefore more conducive to cementation/preservation. The chronostratigraphy of the southern Cape aeolianite record appears to be similar to that found in other major aeolianite localities (e.g., South Australia, Bermuda and Barbados).

The lack of carbonate found in sediments at the transition of OIS 1/2 and OIS 4/5 is not due to leaching. It may reflect increased terrestrially derived quartz sand and/or changes in the positions and strengths of the Benguela and Agulhas currents dampening carbonate production in the near-shore zone from which the sediment for the dunes is sourced. Alternatively, or additionally at times, it may be due to subaerial exposure of coastal platform sediments during preceding sea-level low stands, which allowed carbonate leaching prior to aeolian reworking into the dunes.

The presence of such a thickness of aeolianites is partly interpreted as showing that palaeowave energy levels on the southern Cape coast have been high, building up littoral sediments and that onshore winds have been significant over the long term. It is also suggested that Late Quaternary sea-level oscillations have repeatedly caused the driving onshore of carbonate-rich sediments. Where the coastal platform shelves gently and there are no other topographical obstructions this have led to the formation sheet-like aeolianites. Elsewhere, where the coastal platform shelves steeply away from the present-day coastline, sea level fluctuations repeatedly moved sediment close to the same localities allowing the building up of cordon dunes.

The above aeolianite/cordon dune model of deposition has a number of palaeoenvironmental implications. Unlike the SRZ in the Northern Cape of South Africa, which has shown significant LGM aridity and Aeolian activity (Thomas and Shaw, 2002; Bateman et al., 2003), this cannot have been the case for the WRZ. The lack of LGM ages from the aeolianites and cordon dunes on the southern Cape shows they were not active at this time and that regionally conditions were never arid enough to leave enough sediment exposed for aeolian deflation. This supports Illenberger's (1996) hypothesis that aeolian activity was limited to the littoral zone and did not occur at a regional level as proposed by Malan (1990). Even Cape Agulhas, which presently receives less rainfall than Wilderness, must have generally been well vegetated. Pollen evidence from Wilderness and Vankervelsvlei ~20km further east supports this, as although the period leading up to and including the LGM was generally drier and cooler than present, it was not dry enough to completely replace the forest component with a heath (fynbos) component (Irving and Meadows, 1997; Irving, 1998). It also shows that aeolian deposition in the southern Cape occurred episodically over a much longer time-span than previously postulated, extending beyond interglacials into the early parts of glacials (e.g., OIS 4). The impact of this on palaeoenvironments will have been tempered by the seemingly strong primary control on aeolian activity of sea-level changes. Thus, aeolian activity may not have penetrated more than a few kilometres inland and although only hinted at within the chronostratigraphy, possibly formed during fairly short-lived construction events followed by periods of quiescence and or partial erosion.

Acknowledgements

Mark Bateman and Peter Holmes acknowledge the financial and logistical support of the Sheffield Centre for International Drylands Research and the University of Cape Town. Work undertaken by Andrew Carr was with the financial support of a University of Sheffield studentship and bursaries from the Dudley Stamp Memorial Fund. Paul Coles and Graham Allsopp are thanked for their cartographic assistance. Professors David Thomas, Colin Murray-Wallace are thanked for their comments on this manuscript as are Colin Lewis and an anonymous referee. Professor David Thomas, and Matt Telfer are thanked for their assistance in the field.

References

Aharon, P., Chappell, J., 1986. Oxygen isotopes, sea-level changes and the temperature history of a coral reef environment in New Guinea over the last 10^5 years. Palaeogeography, Palaeoclimatology, Palaeoecology 56, 337–379.

Aitken, M., 1985. Thermoluminescence Dating. Academic Press, London, 359pp.

Avery, G., Cruz-Uribe, K., Goldberg, P., Grine, F.E., Klein, R.G., Lenardi, M.J., Marean, C.W., Rink, J.W., Schwarcz, H.P., Thackeray, A.I., Wilson, M.L., 1997. The 1992–1993 excavations at Die Kelders Middle Stone Age cave site, South Africa. Journal of Field Archaeology 24, 263–291.

Bard, E., Antonioli, F., Silenzi, S., 2002. Duration and timing of the penultimate interglacial sea-level highstand: implications for the astronomical theory of palaeoclimate. Earth and Planetary Science Letters 196, 135–146.

Barrable, A., Meadows, M.E., Hewitson, B.C., 2002. Environmental reconstruction and climate modelling of the Late Quaternary in the winter rainfall region of the western Cape, South Africa. South African Journal of Science 96, 611–616.

Barwis, J.H., Tankard, A.J., 1983. Pleistocene shoreline deposition and sea-level history at Swartklip, South Africa. Journal of Sedimentary Petrology 53, 1281–1294.

Bascomb, C.L., 1974. Physical and chemical analysis of <2mm samples. In: Avery, B.W., Bascomb, C.L. (Eds.), Soil Survey

Laboratory Methods. Soil Survey Technical Monograph 6. Batholomew Press, Harpendon.

Bateman, M.D., Catt, J.A., 1996. An absolute chronology for the raised beach deposits at Sewerby, E. Yorkshire, UK. Journal of Quaternary Science 11, 389–395.

Bateman, M.D., Thomas, D.S.G., Singhvi, A.K., 2003. Extending the aridity record of the Southwest Kalahari: current problems and future perspectives. Quaternary International 111, 37–49.

Birch, G.F., De Plessis, A., Willis, J.P., 1978. Off shore and on land geological and geophysical investigations in the Wilderness Lakes region. Transactions of the Geological Society of South Africa 81, 339–352.

Brooke, B., 2001. The distribution of carbonate eolianite. Earth Science Reviews 55, 135–164.

Chappell, J., Polach, H., 1991. Postglacial sea-level rise from a coral record at Huon Peninsula, Papua New Guinea. Nature 349, 147–149.

Chappell, J., Omura, A., Esat, T., McCulloch, M., Pandolfi, J., Ota, Y., Pillans, B., 1996. Reconciliation of Late Quaternary sea-levels derived from coral terraces at the Huon Peninsula with deepsea oxygen isotope records. Earth and Planetary Science Letters 141, 227–236.

Cohen, A.L., Tyson, P.D., 1995. Sea surface temperature fluctuations during the Holocene off the south coast of Africa: implications for terrestrial climate and rainfall. The Holocene 5, 304–312.

Cowling, R.M., Cartwright, C.R., Parkington, J.E., Allsop, J., 1999.

Fossil wood and charcoal assemblages form Elands Bay Cave, South Africa: implications for Late Quaternary vegetation and climates in the winter rainfall fynbos biome. Journal of Biogeography 26, 367–378.

Davies, O., 1976. The older coastal dunes in Natal and Zululand and their relation to former shorelines. Annals of the South African Museum 71, 19–32.

Deacon, H.J., 1995. Two Late Pleistocene–Holocene archaeological depositories from the southern Cape, South Africa. South African Archaeological Bulletin 50, 121–131.

Deacon, H.J., Deacon, J., 1999. Human Beginnings in South Africa. David Phillip Publishers, Cape Town, 214pp.

Deacon, H.J., Deacon, J., Scholtz, A., Thackeray, J.F., Brink, J.S., Vogel, J.C., 1984. Correlation of palaeoenvironmental data from

the Late Pleistocene and Holocene deposits of Boomplaas Cave, southern Cape. In: Vogel, J.C. (Ed.), Late Cainozoic Palaeoclimates of the Southern Hemisphere. A.A. Balkema, Rotterdam, pp. 339–352.

Dingle, R.V., Rogers, J., 1972a. Effects of sea-level changes on the

Pleistocene palaeoecology of the Agulhas Bank. Palaeoecology of Africa 6, 55–58.

Dingle, R.V., Rogers, J., 1972b. Pleistocene palaeogeography of the Agulhas Bank. Transactions of the Royal Society of South Africa 40, 155–165.

Dingle, R.V., Birch, G.F., Bremner, J.M., DeDecker, R.H., Du Plessis, A., Engelbrecht, J.C., Fincham, M.J., Fitton, B.W., Flemming, B.W., Gentle, R.I., Goodland, S.W., Martin, A.K., Mills, E.G., Moir, G.J., Parker, R.J., Robson, S.H., Rogers, J., Salmon, D.A., Siesser, W.G., Simpson, S.W., Summerhayes, C.P., Westall, F., Winter, A., Woodborne, M.W., 1987. Deep-sea sedimentary environments around southern Africa (South-East Atlantic and South-West Indian Oceans). Annals of the South African Museum 98, 1–27.

Folk, R.L., Ward, W.C., 1957. Brazos River Bar, a study in the significance of grain size parameters. Journal of Sedimentary Petrology 27, 3–26.

Frechen, M., Dermann, B., Boenigk, W., Ronen, A., 2001. Luminescence chronology of aeolianites from the section at Givat Olga- Coastal Plain of Israel. Quaternary Science Reviews 20, 805–809.

Henshilwood, C.S., Sealy, J.C., Yates, R., Cruz-Uribe, K.,Goldberg,

P., Grine, F.E., Klein, R.G., Poggenpoel, C., Van Niekerk, K., Watts, I., 2001. Blombos Cave, southern Cape, South Africa: preliminary report on the 1992–1999 excavations of the middle stone age levels. Journal of Archaeological Science 28, 421–448.

Henshilwood, C.S., d'Errico, F., Yates, R., Jacobs, Z., Tribolo, C., Duller, G.A.T., Mercier, N., Sealy, J.C., Vallada, H., Watts, I.,

Wintle, A.G., 2002. Emergence of modern human behavior: middle stone age engravings from South Africa. Science 295, 1278–1280.

Illenberger, W.K., 1988. The Holocene evolution of the Sunday's Estuary and adjacent coastal dunefields, Algoa Bay, South Africa. In: Dardis, G.F., Moon, B.P. (Eds.), Geomorphological Studies in Southern Africa. A.A Balkema, Rotterdam, pp. 389–405.

Illenberger, W.K., 1996. The geomorphic evolution of the Wilderness dune cordons, South Africa. Quaternary International 33, 11–20.

Illenberger, W.K., Verhagen, B.T., 1990. Environmental history and dating of coastal Dunefields. South African Journal of Science 86, 311–314.

Illenberger, W., Rust, I., Vogel, J., 1997. Luminescence dating of coastal dunes of the southern Cape. XIII Biennial Conference of the Southern African Society for Quaternary Research Abstracts of Papers 6–7.

Irving, S.J., 1998. Late Quaternary palaeoenvironments at Vankervelsvlei, near Kynsna, South Africa. Unpublished M. Sc. Thesis, University of Cape Town.

Irving, S.J., Meadows, M.E., 1997. Radiocarbon chronology and organic matter accumulation at Vankervelsvlei, near Knysna, South Africa. South African Geographic Journal 79, 101–105.

Kocurek, G., 1998. Aeolian system response to external forcing factors—a sequence stratigraphic view of the Saharan region. In: Alsharhan, A.S., Glennie, K.W., Whittle, G.L., Kendall, C.G.St.C. (Eds.), Quaternary Deserts and Climate Change. Balkema, Rotterdam.

Lambeck, K., Chappell, J., 2001. Sea-level change through the last glacial cycle. Science 292, 679–686.

Lambeck, K., Esat, T.M., Potter, E-K., 2002. Links between climate and sea-levels for the past three million years. Nature 419, 199–206.

Lewis, C.A., 1999. Field guide to the Quaternary in the eastern and southern Cape. XV International Congress of the International Union for Quaternary Research.

Malan, J.A., 1987. The BredasdorpGroup in the area between Gans Bay and Mossel Bay. South African Journal of Science 83, 506–507.

Malan, J.A., 1989. Lithostratigraphy of the Waenhuiskrans Formation (BredasdorpGroup). South African Committee for Stratigraphy (SACS), Lithostratigraphic Series Number 8, Department of Mineral and Energy Affairs.

Malan, J.A., 1990. The stratigraphy and sedimentology of the Bredasdorp Group, Southern Cape Province. Unpublished M.Sc. Thesis, University of Cape Town.

Malan, J.A., Viljoen, J.H.A., 1990. Mesozoic and Cenozoic geology of the Cape South coast. Guidebook Geocongress '90. Geological Society of South Africa PO3, 1–81.

Martin, A.R.H., 1959. The stratigraphy and history of Groenvlei, a South African coastal fen. Australian Journal of Botany 7, 142–167.

Martin, A.R.H., 1962. Evidence relating to the Quaternary history of the Wilderness lakes. Transactions of the Geological Society of South Africa 65, 19–45.

Meadows, M.E., Baxter, A.J., 1999. Late Quaternary palaeoenvironments of the southwestern Cape, South Africa: a regional synthesis. Quaternary International 57–8, 193–206.

Murray, A.S., Wintle, A.G., 2000. Luminescence dating of quartz using an improved single-aliquot regenerative-dose protocol. Radiation Measurements 32, 57–73.

Pirazolli, P.A., Radtke, U., Hatoro, W.S., Jouannic, C., Hoang, C.T., Causse, C., Best, M.B., 1991. Quaternary raised coral-reef terraces on Sumba Island, Indonesia. Science 252, 1834–1836.

Potgieter, C.T., 1950. The structure and petrology of the George granite plutons and invaded Pre-Cape sedimentary rocks. Annals of the University of Stellenbosch 26, 323–412.

Prescott, J.R., Hutton, J.T., 1994. Cosmic ray contributions to dose rates for luminescence and ESR dating: large depths and long-term time variations. Radiation Measurements 23, 497–500.

Ramsay, P.J., 1995. 9000 years of sea-level change along the Southern African coastline. Quaternary International 31, 71–75.

Ramsay, P.J., Cooper, J.A.G., 2002. Late Quaternary sea-level change in South Africa. Quaternary Research 57, 82–90.

Roberts, D., Berger, L., 1997. Last Interglacial (c. 117 kyr) human footprints from South Africa. South African Journal of Science 93, 349–354.

Shaw, A.E., Holmes, P.J., Rogers, J., 2001. Depositional landforms and environmental change in the headward vicinity of Dias Beach, Cape Point. South African Journal of Geology 104, 101–114.

Siesser, W.G., 1970. Carbonate components and mineralogy of the South African coastal limestones and linstones of the Agulhas Bank. Transactions of the Geological Society of South Africa 73, 49–63.

Siesser, W.G., Rogers, J., 1970. An investigation of the suitability of four methods used in routine carbonate analysis of marine sediments. DeepSea Research 18, 135–139.

Tankard, A.J., Schweitzer, F.R., 1974. The geology of Die Kelders Cave and environs: a palaeoenvironmental study. South African Journal of Science 70, 365–369.

Tankard, A.J., Schweitzer, F.R., 1976. Textural analysis of cave sediments: Die Kelders, Cape Province, South Africa. In: Davidson, D.A., Shackley, M.L. (Eds.), Geoarchaeology: Earth Science and the Past. Duckworth, London, pp. 289–316.

Thomas, D.S.G., Shaw, P.A., 2002. Late Quaternary environmental change in central southern Africa: new data, synthesis, issues and prospects. Quaternary Science Reviews 21, 783–797.

Thomas, D.S.G., O'Connor, P., Bateman, M.D., Shaw, P.A., Stokes, S., Nash, D.J., 2000. Dune activity as a record of Late Quaternary aridity in the northern Kalahari: new evidence from the northern Namibian interpreted in the context of regional arid and humid chronologies. Palaeogeography Palaeoclimatology Palaeoecology 156, 243–259.

Tinley, K.L., 1985. Coastal dunes of South Africa. South African National Scientific Programmes Report No. 109, Foundation for Research Development Council for Scientific and Industrial Research, Pretoria, 300pp.

Tyson, P.D., 1971. Outeniqualand: the George-Knysna area. The South African landscape, No. 2, South African Geographical Society, 3–23.

Van Andel, T.H., 1989. Late Pleistocene sea levels and the human exploitation of the shore and shelf of southern South Africa. Journal of Field Archaeology 16, 133–155.

Vogel, J.C., Wintle, A.G., Woodbourne, S.M., 1999. Luminescence dating of coastal sands: overcoming changes in environmental dose rate. Journal of Archaeological Science 26, 729–733.

Yokoyama, Y., Lambeck, K., De Deckker, P., Johnston, P., Fifield, L.K., 2000. Timing of the Last Glacial Maximum from observed sea-level minima. Nature 406, 713–716.

Zhou, L., Williams, M.A.J., Peterson, J.A., 1994. Late Quaternary aeolianites, palaeosols and depositional environments on the Nepean Peninsula, Victoria, Australia. Quaternary Science Reviews 13, 225–239.